Erschienen in: Energy Procedia ; 77 (2015). - S. 687-693
https://dx.doi.org/10.1016/j.egypro.2015.07.098

Available online at www.sciencedirect.com

ScienceDirect

Energy Procedia 77 (2015) 687 – 693

Energy Procedia

5th International Conference on Silicon Photovoltaics, SiliconPV 2015

Effect of Al concentration analyzed by ICP-OES on the structural, electrical and optical properties of co-sputtered ZnO:Al films

Angelika Gorgulla, Dominik P. Ertel, Michael Steyer, Giso Hahn, Barbara Terheiden

University of Konstanz, Department of Physics, P.O. Box X916, D-78457 Konstanz, Germany

Abstract

We prepare co-sputtered Al doped zinc oxide (ZnO:Al) films and investigate the effect of elemental concentrations on the electrical, optical and structural film properties by varying the rf-power applied to the Al target P_{Al}. To obtain the Zn and Al concentrations Inductively Coupled Plasma Optical Emission Spectrometry (ICP-OES) is used, a novel and relatively simple approach for a high throughput investigation of elemental concentrations in ZnO films. It is found, that while the Al concentration c_{Al} rises exponentially from $1.4 \cdot 10^{20}$ to $7.2 \cdot 10^{20}$ cm^{-3} with increasing P_{Al}, the charge carrier density increases only linearly from $2.9 \cdot 10^{19}$ to $1.2 \cdot 10^{20}$ cm^{-3}. For $P_{Al} > 150$ W this can be attributed to an increased doping induced defect density. For $P_{Al} > 250$ W, the enhanced bombardment of the growing surface with highly energetic particles from the plasma leads to more structural disorder and reduced crystallinity, which results in a decrease of mobility and of charge carrier density. Atomic force microscopy (AFM) images show a correlation between crystallite size and surface roughness of the films, suggesting that larger crystallite sizes promote a smoother film surface. The optical bandgap widens from 3.26 to 3.37 eV with increasing Al concentration due to the Burstein-Moss-Effect, which causes a blue-shift of the absorption edge. In the long wavelength range ($\lambda > 1000$ nm), the optical transmission decreases with increasing Al concentration due to enhanced free carrier absorption. An Al rf-power of 200-250 W is found for films with the best combination of low resistivity and high transmission.

© 2015 The Authors. Published by Elsevier Ltd. This is an open access article under the CC BY-NC-ND license (http://creativecommons.org/licenses/by-nc-nd/4.0/).
Peer review by the scientific conference committee of SiliconPV 2015 under responsibility of PSE AG

Keywords: ZnO:Al, AZO, TCO, ICP-OES, Magnetron Sputtering, Rf-Power, Elemental Concentrations, HJC

1. Introduction

Transparent conductive ZnO:Al thin films are of interest in numerous photovoltaic applications, e. g. a-Si:H/c-Si heterojunction and thin film solar cells, due to their features such as a high transmittance above 85% within the UV, VIS and NIR as well as low electrical resistivity in the order of 10^{-3} to 10^{-4} Ωcm. The most commonly used deposition technique is rf magnetron sputtering. In this study, we prepared co-sputtered ZnO:Al films with varying

Konstanzer Online-Publikations-System (KOPS)
URL: http://nbn-resolving.de/urn:nbn:de:bsz:352-0-304202

1876-6102 © 2015 The Authors. Published by Elsevier Ltd. This is an open access article under the CC BY-NC-ND license (http://creativecommons.org/licenses/by-nc-nd/4.0/).
Peer review by the scientific conference committee of SiliconPV 2015 under responsibility of PSE AG
doi:10.1016/j.egypro.2015.07.098

the rf-power applied to the Al target (Al rf-power) P_{Al} from 300 to 350 W and investigated its effect on the elemental concentrations in association with their impact on the structural, optical and electrical film properties. To obtain the Al and Zn concentrations, Inductively Coupled Plasma Optical Emission Spectrometry (ICP-OES) was used, which is a novel approach for investigating elemental concentrations in ZnO thin films. ICP-OES is a chemical method commonly used for the detection of trace-level elements based on an inductively coupled plasma producing excited atoms and ions, which emit electromagnetic radiation at element specific wavelengths. The intensity of the characteristic emission lines allows to determine the concentration (atoms per volume) of the element within the sample [1].

2. Experiment

ZnO:Al films were deposited on float zone (FZ) Si wafers (for ellipsometry measurements) and borofloat glass (for all remaining measurements) at room temperature in a rf-13.56 MHz magnetron sputtering system (ATC-2200, AJA International). For film deposition metallic Zn and Al targets (99.99% pure) have been used.

Prior to the sputtering process, all substrates were ultrasonically cleaned in acetone, isopropanol and deionized water sequentially. Before deposition, the sputtering chamber was evacuated to a base pressure of $<10^{-6}$ Torr. After a pre-sputtering period of 2 min under deposition conditions, the sputtering deposition was performed at a rf -power of 5 W and a pressure of 2.5 mTorr for ZnO:Al deposition. Argon (20 sccm) was used as sputtering and oxygen (6 sccm) as reaction gas. During deposition, the substrates were rotated with constant speed for film uniformity.

Electrical resistivity, free carrier density and carrier mobility of the films were derived from Hall measurements (HMS-5000, Ecopia) at room temperature using the van der Pauw method. Optical properties were characterized by spectral transmission and reflection measurements within a wavelength range of 300-2500 nm taken by a spectral photometer (Cary 5E, Varian).

The optical constants are deduced from spectral ellipsometry measurements (V-VASE, J.A. Woollam Co. Inc.) between wavelengths from 250 to 1000 nm. For this purpose the (ψ, Δ) data were fitted by a Kramers-Kronig-consistent model [2]. The optical band gap E_{gap} was calculated from the fitted data by using Tauc's formula [3]. The crystalline structure of the films was analyzed by X-Ray Diffraction (XRD) (D8 XRPD, Bruker) using Cu K_{α} radiation (0.1542 nm). The surface morphology was evaluated by means of atomic force microscopy (AFM) (MFP-3D-SA, Asylum Research). The ratio of Zn to O atoms was determined by SEM-EDX. For ICP-OES (720 series, Agilent) elemental analysis, the ZnO:Al films were dissolved in $0.5\%_{abs}$ hydrofluoric acid. To guarantee accurate ICP-OES measurements with elemental concentrations above quantification limit, the thicknesses of the deposited films were in the range of 800-1500 nm, as determined by profilometric measurements. In order to verify the accurateness of the ICP-OES analysis, an external GD (Glow Discharge)-OES measurement of one sample was performed by Spectruma Analytic GMBH.

3. Results

3.1 Structural properties

The films exhibit two major diffraction peaks at around 34.6 and 35.8°, which can be assigned to reflections from (002) and (101) planes, respectively, of the hexagonal wurtzite phase of zinc oxide [4] (Fig. 1 left). The intensity of the diffraction peaks increases up to $P_{Al} = 250$ W and decreases for higher Al rf-power. Same trend can be observed for the mean crystallite size derived from peak position and the full width at half maximum (FWHM) according to Scherrer's equation [5] (Fig. 1 right). The uncertainty in crystallite size calculation is assumed to be less than 5% [6].

For $P_{Al} < 250$ W, the degradation of the crystallographic structure can be attributed to insufficient kinetic energy of the sputtered atoms in order to obtain optimal bonding configuration with the adjacent substrate and film atoms, which can also cause nucleation on the film surface. For $P_{Al} > 250$ W the degradation of crystallinity can be attributed to an increased bombardment of the growing films with very highly energetic particles from the plasma.

To analyze the impact of Al rf-power on the surface morphology of the films AFM images have been recorded (Fig. 2). The root mean square (RMS) roughness decreases from 3.7 to 0.8 nm as P_{Al} is increased from 50 to 250 W

and increases for higher P_{Al} up to 2.4 nm. This trend is inversely proportional to the crystallite size, which suggests that larger crystallite sizes promote smoother film surfaces.

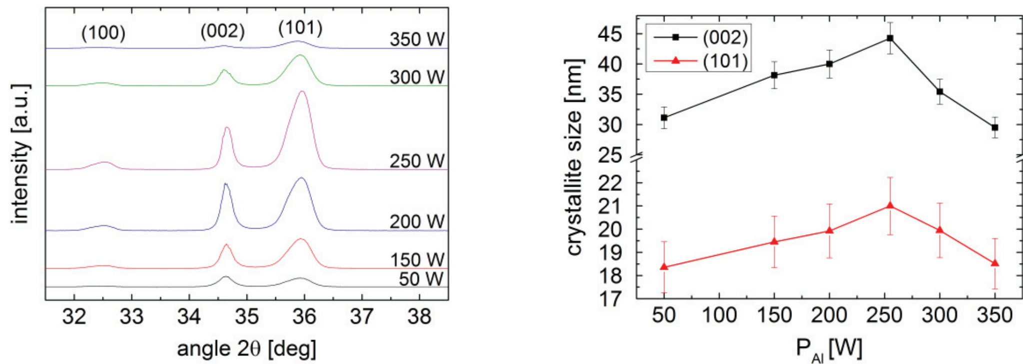

Fig. 1. XRD spectra (left) and crystallite sizes derived by Scherrer's equation (right) in dependence of Al rf-power.

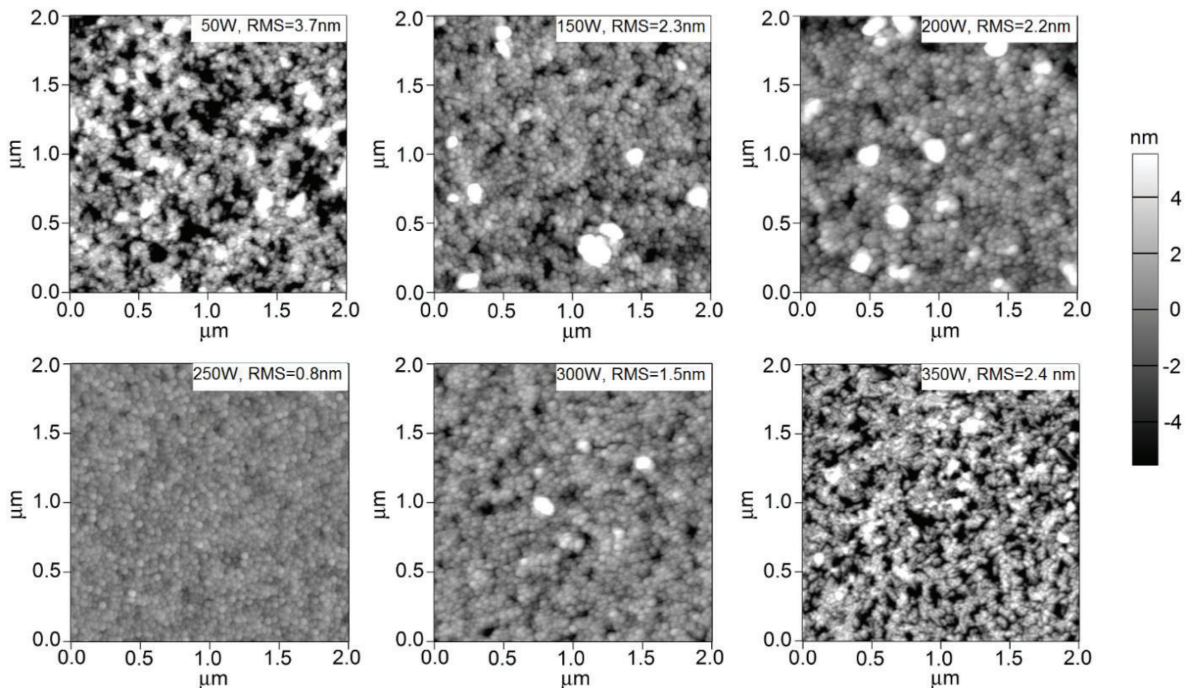

Fig. 2. AFM images of ZnO:Al films deposited on glass with various Al rf-powers. The RMS surface roughness is inserted within the graphs.

3.2 Elemental concentrations and electrical properties

Al concentration c_{Al} and charge carrier density N_e in dependence of Al rf-power are shown in Fig. 3 left. The Al concentration increases exponentially with increasing P_{Al} from $1.4\cdot10^{20}$ to $7.2\cdot10^{20}$ cm^{-3}, which corresponds to an increase of Al doping concentration from 0.3 to 2.0 at.%. This increase, however, can only partly be attributed to an enhanced sputtering rate from the Al target, which increases linearly from 0.56 nm/s at 50 W to 0.62 nm/s at 350 W (not shown). As a consequence of free electrons released by the substitution of Al^{3+} ions at the sites occupied by Zn^{2+} ions, the increase in Al concentration increases the charge carrier density. However, the free carrier density

does not increase proportional to the c_{Al}, which means that not every Al atom effectively contributes a free carrier.

This becomes more clearly when the fraction of Al atoms effectively acting as dopants, which is given by the ratio N_e/c_{Al}, is plotted over rf Al power (Fig. 3 right). As P_{Al} is increased from 50 to 150 W, the N_e/c_{Al} increases from 0.23 to 0.41, presumably since more Al atoms sputtered from the target can acquire sufficient kinetic energy in order to obtain optimal bonding configuration with the adjacent substrate and film atoms and subsequently act as dopants. As P_{Al} is further increased from 150 to 350 W, however, N_e/c_{Al} decreases from 0.41 to 0.15. There are two possible explanations: firstly, an increased fraction of Al atoms is not incorporated in the ZnO matrix as dopants, e.g. as substitutional atoms on Zn lattice sites, but rather as interstitials inducing defects. Secondly, an increased fraction of charge carriers introduced by Al dopants is compensated by other defects, e.g. as a result of poor crystallinity. In any case, the ratio N_e/c_{Al} can be considered as a measure for the defect density within the films.

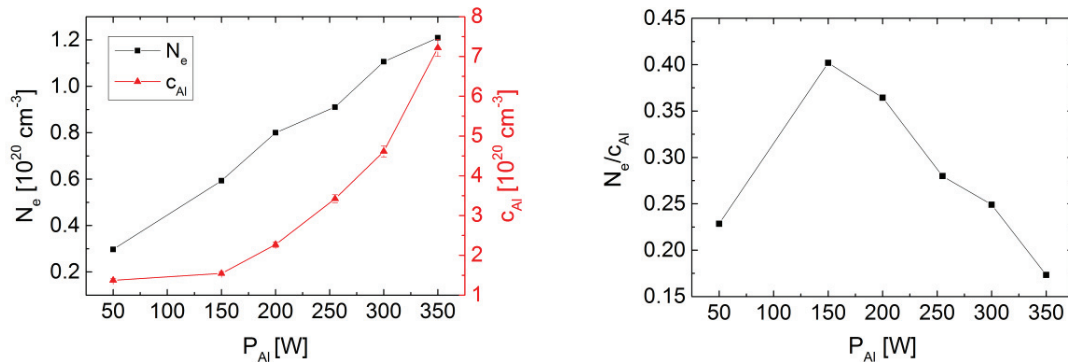

Fig. 3. Al concentrations c_{Al} and charge carrier density N_e (left) and fraction of Al atoms effectively acting as donors N_e/c_{Al} (right) versus Al rf-power. The statistical error of N_e is 1%.

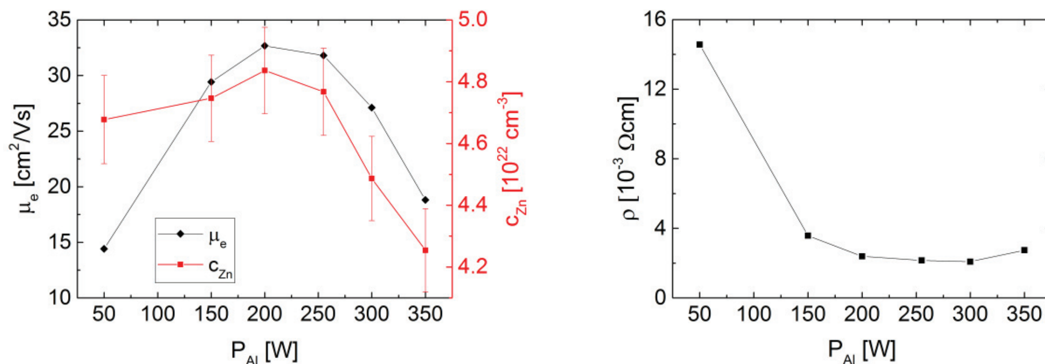

Fig. 4. Mobility μ_e and Zn concentration c_{Zn} (left) and electrical resistivity ρ (right) versus Al rf-power. The statistical errors of μ_e and ρ are below 1%.

The Zn concentration c_{Zn} and charge carrier mobility μ_e in dependence of Al rf-power are shown in Fig. 4 left. The ratio of Zn to O atoms is about 52:48 in all films, as measured by EDX. Therefore, the decrease of c_{Zn} for $P_{Al} > 200$ W is due to a decrease in film density, as the films are grown closer to the amorphous/microcrystalline regime (compare section 3.1). For $P_{Al} \geq 150$ W the free charge carrier mobility is correlated to the Zn concentration. The drop in μ_e at Al rf-power below 150 W can be attributed to both enhanced defect scattering and grain boundary scattering due to the increased defect density and decreased crystallite sizes, respectively. The decrease in mobility above 200 W can mainly be explained by enhanced defect scattering due to the increase of doping induced defects. Above 250 W, enhanced grain boundary scattering due to smaller crystallite sizes contributes to the strong degradation of the mobility. The electrical film quality can also be affected by the surface roughness: an increase in surface roughness facilitates oxygen absorption on the film surface, which leads to the formation of dangling bonds

acting as electron traps [7]. Besides that, chemisorption of acceptor oxygen on the surface can form an electronic depletion layer, which acts as a surface barrier and thereby reduces the mobility [8]. Adsorbed oxygen may therefore also contribute to the decreases of Ne/cAl and mobility at PAl > 250 W.

The electrical resistivity ρ, which is proportional to the reciprocal of carrier concentration and mobility, decreases from $1.5 \cdot 10^{-2}$ Ωcm at 50 W to below $4 \cdot 10^{-3}$ Ωcm at higher Al rf-power (Fig. 4 right). For solar cell applications, e. g. in heterojunction solar cells transparent conductive top layers serving as anti-reflection coating, a thickness of the ZnO:Al film of around 80 nm is required. Decreasing the thickness of our films to 80 nm leads to an increase of resistivity by a factor of two due to a decrease in charge carrier density as well as in mobility. The reason is that as the film thickness increases, the structural disorder decreases and crystallite sizes become larger [9].

The ICP-OES analysis was confirmed by external GD-OES for one sample at $P_{Al} = 350$ W, which resulted in a deviation of less than 3% in the Al doping concentration. The GD-OES measurements showed homogenously distributed Al, Zn and O concentrations with elemental concentrations of about 1%, 51% and 48%, respectively.

3.3 Optical properties

Optical transmittance spectra for various P_{Al} are depicted in Fig. 5 left. Bare borofloat glass is shown as reference. The highest optical transmission within the VIS-range is obtained at 250W and the lowest at 350 W. In the long wavelength range (λ > 1000 nm) the optical transmission decreases significantly with increasing Al concentration as a consequence of enhanced free carrier absorption. In Fig. 5 right, optical reflectance spectra are shown. It is found that in the long wavelength range (λ > 1000 nm) the total reflectance for ZnO thin film decreases with increasing the Al concentration. The optical bandgap (Fig. 6 left) widens with increasing P_{Al} due to the Burstein-Moss-Effect. The optical transmittance weighted by ASTM G173-03 solar spectrum within a wavelength range relevant for solar cells (300-1100 nm) is depicted in Fig. 6 left. The band gap widening leads to an increase of the weighted transmission in the range of 150-250 W. The highest weighted transmission with 73% is achieved at 250 W. For $P_{Al} > 250$ W the weighted transmission decreases slightly as the free carrier absorption becomes more pronounced in the transmission spectra. The film deposited at a very high Al rf-power of 350 W exhibits a significantly lower transmission within the whole wavelength range as consequence of a more pronounced metallic character.

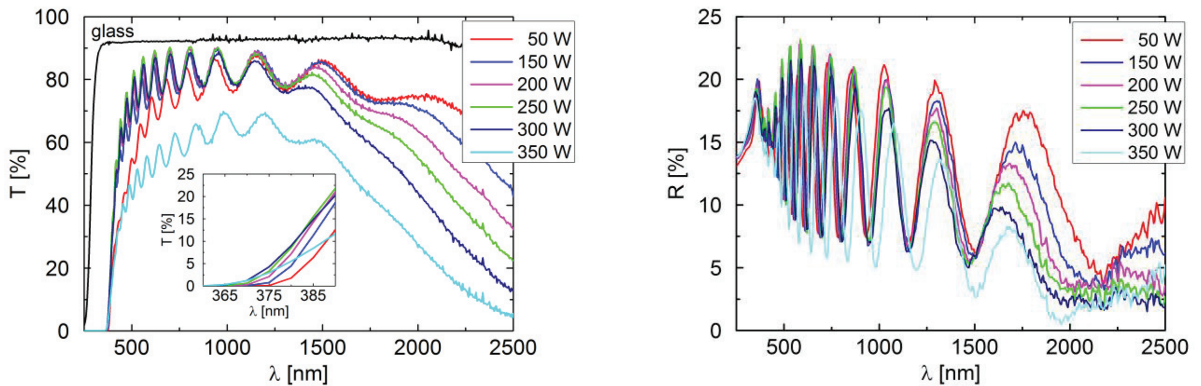

Fig. 5. Optical transmission (left) and reflectance (right) spectra for various Al rf-powers.

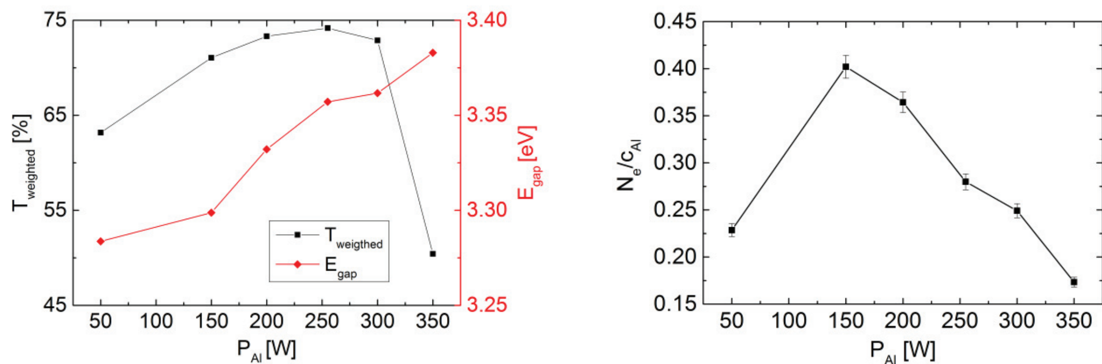

Fig. 6. Optical transmission weighted by ASTM G173-03 solar spectrum in the range of 300-1100 nm and optical band gap (left) and Haacke's figure of merit (right) in dependence of Al rf-power.

A figure of merit Φ_{TC} for transparent conductive materials defined by Haacke $\Phi_{TC} = (T_{550})^{10}/R_{Sh}$ [10], where T_{550} is the optical transmission at 550 nm and R_{Sh} the sheet resistance, was determined for all films in order to obtain a quantitative measure for optoelectronic performance (Fig. 6 right). For heterojunction solar cell application, the figure of merit should exceed 8.0 mΩ. This is achieved at a rf Al power of 200-250 W, where the films with highest mobility and best structural quality are deposited. The corresponding Al doping concentrations range from 2.3 to $3.4 \cdot 10^{20}$ cm^{-3} and 0.54 to 0.84 at.%, respectively.

4. Summary

ICP-OES is a novel and relatively simple approach for a high throughput investigation of elemental concentrations in ZnO films. The accuracy of ICP-OES was confirmed by an external GD-OES measurement for one sample, which resulted in a deviation of less than 3% in the Al doping concentration. The ICP-OES analysis has shown that the Al concentration within the films increases exponentially with increasing P_{Al}. The charge carrier density, however, does increase linearly, as with increasing Al concentration the fraction of Al atoms effectively acting as dopants decreases. This can be attributed to an increased doping induced defect density above 150 W. XRD measurements showed, that an Al rf-power below 250 W leads to a degradation in crystallinity due to insufficient kinetic energy of the sputtered atoms, which results in a significantly reduced mobility. For $P_{Al} > 250$ W, on the other hand, enhanced bombardment of the growing surface with highly energetic particles from the plasma leads to more structural disorder and reduced crystallinity and results in decrease of mobility as well as of charge carrier density.

AFM images have shown a correlation between crystallite sizes and RMS surface roughness of the films, suggesting that larger crystallite sizes promote a smoother film surface. As increased surface roughness facilitates O_2 chemisorption it can contribute to degradation of the electrical film properties above and below 250 W.

The Al concentration also has a significant impact on the optical film properties. The optical bandgap widens from 3.26 to 3.37 eV with increasing Al concentration due to the Burstein-Moss-Effect, which causes a blue-shift of the absorption edge. In the long wavelength range ($\lambda > 1000$ nm), the optical transmission decreases with increasing Al concentration due to enhanced free carrier absorption. In the wavelength range relevant for solar cells (300-1100 nm) the highest weighted transmission of 73% is obtained at 250 W. According to Haacke's figure of merit, films with best optoelectronic quality are deposited at 200-250 W.

Acknowledgements

Part of this work was financially supported by the German Federal Ministry for the Environment, Nature Conservation and Nuclear Safety (FKZ 0325581) and within the "REFINE" project from the Carl-Zeiss-Stiftung. The content is the responsibility of the authors.

References

[1] Ghosh S, Prasanna VL, Sowjanya B, Srivani P, Alagaraja M, Banji D. Inductively Coupled Plasma - Optical Emission Spectroscopy: A Review. Asian Journal of Pharmaceutical Analysis. 2013;3:24-33.
[2] Fox M. Optical Properties of Solids. 2nd ed. Oxford: Oxford University Press; 2010.
[3] Tauc J, Menth A. States in the gap. Journal of Non-Crystalline Solids. 1979;8:569-85.
[4] Miccoli L, Spampinato R, Marzo F, Prete P, Lovergine N. DC-magnetron sputtering of ZnO:Al films on (00.1) Al_2O_3 substrates from slip-casting sintered ceramic targets. Applied Surface Science. 2014;313:418-423.
[5] Scherrer P, Bestimmung der Größe und der inneren Struktur von Kolloidteilchen mittels Röntgenstrahlen. Göttinger Nachrichten Gesellschaft. 1918;2:98-100.
[6] Alexander L, Klug, HP. Determination of Crystallite Size with the X-Ray Spectrometer. Journal of Applied Physics. 1950;21:137-142.
[7] Oh, B Jeong M, Lee W, Myoung J. Properties of transparent conductive ZnO:Al films prepared by co-sputtering. Journal of Crystal Growth. 2005;274:453–57.
[8] Igasaki A, Saito H. The effects of zinc diffusion on the electrical and optical properties of ZnO:Al films prepared by r.f. reactive sputtering. Thin Solid Films. 1991;199:223-30.
[9] Tüzemen EŞ , Eker S, Kavak H, Esen R. Dependence of film thickness on the structural and optical properties of ZnO thin films. Applied Surface Science. 2009;255:6195-200.
[10] Haacke G. New figure of merit for transparent conductors. Journal of Applied Physics. 1976;47:4086-98.